MINISTRY OFINDUSTRY AND TRADE

HANOI UNIVERSITY OF INDUSTRY

NGUYEN HONG TIEN

IMPROVING THE WEAR RESISTANCE OF HIGH-LOAD SCREW PRESSES BY INTEGRATED DESIGN AND HVOF COATING SOLUTIONS

Major: Mechanical Engineering

Major code: 9520103

SUMMARY OF DESERTATION IN

Hanoi - 2026

This desertation has been completed at:

HANOI UNIVERSITY OF INDUSTRY

Scientific supervisors:

1. Assoc. Prof, PhD. Nguyen Tuan Linh – Hanoi University of Industry

2. PhD. Nguyen Van Thien – Hanoi University of Industry

Reviewer 1: Professor, Doctor Nguyen Duc Toan

Reviewer 2: Assoc. Prof, PhD. Le Van Tao

Reviewer 3: Assoc. Prof, PhD. Tran Van Dua

The desertation was defended at the Doctoral Evaluating Council at University level, held at Hanoi University of Industry at …., date….. 2026

The desertation can be found at:

- The library of Hanoi University of Industry
- Vietnam National Library

INTRODUCTION

High-load screw presses are key components in bulk material processing lines, responsible for compressing, shaping, and conveying materials under high pressure. In the production of clean charcoal from sawdust, the screw press plays a decisive role in determining bonding strength, density, and overall product quality. However, harsh operating conditions involving high pressure, intense friction, and elevated temperatures lead to rapid wear of the screw, reducing service life, increasing maintenance costs, and negatively affecting productivity. This doctoral research focuses on solutions to improve the wear resistance of high-load screw presses through optimized geometric design, numerical simulation, and the application of combined high-velocity oxygen fuel (HVOF) thermal spray coating technology, with the aim of extending service life, reducing costs, and enhancing operational efficiency.

The dissertation aims to optimize the design of high-load screw presses and to master HVOF coating technology in order to improve wear resistance in clean charcoal production. The research object is a high-load screw press used for compressing and conveying sawdust under conditions of high pressure and friction, where severe wear and deformation are likely to occur. The study integrates geometric optimization, numerical simulation of material flow and wear, and surface coating using the HVOF method to enhance screw durability. The research has scientific significance in that it is among the first to establish a comprehensive integrated simulation model capable of accurately predicting wear-prone regions and proposing effective solutions to enhance wear resistance. It also contributes to the theoretical foundation of mechanical equipment simulation involving bulk materials and expands applications in component design and service life prediction. The practical significance of the research is reflected in extending component lifespan, reducing maintenance costs, improving production efficiency, and enhancing the competitiveness of enterprises. The research methodology includes theoretical analysis for geometric optimization of the screw, numerical simulation based on the discrete element method, experimental investigation of advanced surface treatment technologies, and the combination of evaluation and model calibration to propose optimal solutions. The dissertation is structured into four chapters. **Chapter 1** presents an overview of high-load screw presses, operating conditions, wear mechanisms, and HVOF coating technology. **Chapter 2** focuses on geometric design optimization of the screw

and numerical simulation of the bulk material compression process to predict pressure distribution, compressive forces, and wear-prone regions. **Chapter 3** introduces the materials, experimental equipment, and experimental results related to coating microstructure and hardness. **Chapter 4** presents experimental testing, analysis, and evaluation of the wear resistance performance of high-load screw presses, with comparisons to simulation results for model validation. The study offers novel contributions by developing an integrated framework for design-simulation-wear prediction, proposing a method for identifying localized wear regions, selecting appropriate HVOF coating parameters, and introducing a new screw press design with enhanced service life, reduced costs, and improved efficiency in clean charcoal production.

CHAPTER 1. LITERATURE REVIEW ON HIGH-LOAD SCREW PRESSES

Chapter 1 presents a comprehensive overview of high-load screw presses, which are critical mechanical components in bulk material processing and manufacturing lines, responsible for compacting, shaping, and conveying materials under high pressure. A screw press typically consists of a screw shaft and helical flights, and is divided into three functional zones: the feeding zone, the compression zone, and the forming zone. As the screw rotates, the material is transported along the axial direction while the volume between successive flights gradually decreases, leading to an increase in pressure, temperature, and material density. As a result, the final product exhibits high bonding strength, compactness, and favorable mechanical properties. In clean charcoal production from sawdust, the screw press is a decisive component that directly affects briquette quality, including burning duration, low smoke emissions, and overall usability. However, continuous operation under high loads, severe friction, and elevated temperatures makes the screw press highly susceptible to wear, deformation, and loss of its working profile, which in turn shortens service life, increases maintenance costs, and reduces production efficiency.

The theoretical basis for screw press design emphasizes key operating parameters such as throughput, pressure, compressive force, torque, compression ratio, and compression chamber length. These parameters govern compaction capability, conveying speed, and energy efficiency. Traditional screw press design methods are largely based on semi-empirical formulas, practical experience, and basic geometric ratios (such as L/D ratio, screw pitch, and helix angle). While these approaches allow rapid calculations, they fail to accurately capture the complex interactions between the bulk material and the screw surface, particularly under severe compression conditions. In contrast, modern non-traditional approaches combine numerical simulation techniques (such as FEM and DEM) with optimization methods (the Taguchi method and genetic algorithms, GA). These approaches enable detailed analysis of stress, deformation, temperature, material flow, friction, and wear prediction, thereby facilitating geometric optimization of the screw to improve performance and reduce wear. In particular, the Discrete Element Method (DEM) offers significant advantages in simulating bulk material flow, as it can explicitly describe particle collisions, compaction, friction, and force distribution among

particles, while accurately predicting localized wear regions on the screw surface - capabilities that FEM and conventional methods struggle to achieve.

In addition to geometric design optimization, surface engineering is a crucial solution for enhancing the wear resistance of screw presses. Surface treatment methods such as electroplating, thermochemical treatments, plasma spraying, vacuum spraying, and cold spraying have been applied, but they still exhibit limitations in terms of coating adhesion and load-bearing capacity. Among these technologies, high-velocity oxygen fuel (HVOF) thermal spraying stands out due to its ability to produce WC-Co or WC-CoCr coatings with high hardness, dense microstructure, excellent adhesion, and superior resistance to wear and corrosion. HVOF coatings are particularly suitable for components operating in harsh environments such as high-load screw presses, where high pressure and intense friction occur continuously. The combination of optimized screw design with HVOF surface coatings significantly extends service life, reduces maintenance costs, stabilizes production, and improves product quality.

An overview of international research indicates that numerous studies have focused on the design, optimization, and simulation of screw conveyors, extruders, mixers, and presses, employing advanced methods such as DEM, FEM, and GA to enhance performance. However, most existing studies primarily address screws operating under moderate loads or with non-cohesive materials, and pay limited attention to high-load screw presses working in harsh environments with highly abrasive bulk materials such as sawdust. Moreover, only a few studies have simultaneously integrated optimized geometric design, DEM-based wear prediction, and advanced surface treatment technologies within a unified research framework.

In Vietnam, several studies have investigated the influence of screw geometry on pressing efficiency and product quality, while others have applied genetic algorithms to optimize screw profiles for clean charcoal production. Nevertheless, these studies are largely limited to isolated experimental investigations and have not incorporated DEM simulations for wear prediction, nor have they implemented advanced coating technologies for screw presses. Meanwhile, although HVOF surface treatment has been studied in certain industrial applications, its use in high-load screw press systems remains limited.

In conclusion, Chapter 1 highlights the necessity of researching solutions to improve the wear resistance of high-load screw presses, driven by practical demands in clean charcoal production and related industries. The comprehensive approach adopted in this dissertation optimized geometric design, DEM-based simulation for material flow analysis and wear prediction, and HVOF coating technology to enhance wear resistance and extend service life. This approach not only meets scientific research requirements but also offers significant practical value, providing a solid foundation for the design, simulation, and experimental investigations presented in the subsequent chapters.

CHAPTER 2. RESEARCH ON DESIGN AND SIMULATION SOLUTIONS TO IMPROVE THE WEAR RESISTANCE OF HIGH-LOAD SCREW PRESSES

Chapter 2 focuses on the optimization of high-load screw press design and the numerical simulation of the bulk material pressing process. The operating behavior of a high-load screw press is influenced by several key factors, including compressive pressure, compression volume, temperature, and pressing time. Among these, compressive pressure and compression volume are the two most critical factors, as they are directly related to the wear level of the screw. Therefore, it is necessary to design the screw profile in such a way that pressure is generated rapidly within the material while simultaneously reducing friction between the material flow and the screw surface. This ensures stable material transport throughout the pressing process and minimizes wear of the component.

The compression volume is determined based on the assumption that the space between the leading flank, groove bottom, and trailing flank of the screw groove is completely filled with material. This volume represents the amount of material conveyed per unit axial length of the screw. The geometric parameters of the screw - including the leading angle α_1, trailing angle α_2, fillet radii R_1 and R_2, screw pitch s, flight crest width e, and groove depth h - govern the magnitude of this volume. Axial variation of the compression volume can be achieved by adjusting the outer diameter of the screw (forming a conical screw), varying the groove depth (using a conical core), or modifying the screw pitch. The combination of these geometric variations allows a suitable compression ratio to be achieved, thereby improving pressing efficiency and reducing wear.

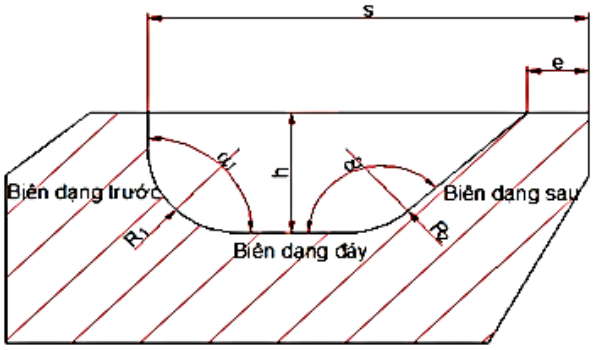

Figure 1: Screw press profile (longitudinal section)

The compressive pressure in a screw press depends on multiple factors, including the initial pressure of the material, screw length, friction

coefficients between the material and the pressing chamber as well as between the material and the screw flights, and the friction angle. The angles defining the screw profile - at the outer surface, within the groove, and at the groove bottom - also play a crucial role in determining the pressure distribution along the screw. These angles are defined based on the relationship between screw pitch and diameter at different axial positions.

This study establishes a method for determining the profile of a high-load screw press by applying a genetic algorithm combined with a weighted-sum approach to solve a multi-objective optimization problem. Two primary objectives are considered: compression volume and compressive pressure. During optimization, the screw profile is treated as an objective function simultaneously dependent on these two factors. Increasing the compression volume improves throughput but reduces pressure; conversely, increasing pressure enhances bonding among bulk material particles but decreases volume and increases friction, leading to accelerated wear. Because these objectives are inherently conflicting, the weighted-sum method is employed to construct a composite objective function while imposing constraints based on actual operating conditions. The design variables in the optimization problem include the leading angle α_1, trailing angle α_2, leading fillet radius R_1, trailing fillet radius R_2, and groove depth h. The optimization program was implemented in MATLAB using a multi-objective optimization toolbox, with crossover rates ranging from 60% to 80%, mutation rates from 2% to 5%, and a total of 800 generations to identify optimal parameter sets. Boundary conditions were selected according to the actual operating parameters of the screw press, with an outer diameter D = 66 mm, inner diameter d = 36 mm, and flight crest width e = 8 mm. The optimization results yielded three different screw profile configurations. In the first case, the compressive pressure increases most slowly, and the pressure distribution along the screw profile is highly non-uniform, leading to localized wear concentrated at the thread roots, particularly in the last three flights, which degrades the operational performance of the screw. In the second case, the pressure increases more rapidly and the compaction capability is improved; however, the screw angles hinder material movement to the next pitch, resulting in increased friction and wear concentrated mainly on the trailing side of the profile. The third case exhibits the fastest pressure increase, smoother material conveying behavior, and a more uniform distribution of wear, thereby reducing localized wear phenomena. Based on the analysis of these three cases, the third configuration is evaluated

as the optimal solution, as it ensures high compressive pressure, effective material transport, and a balanced wear distribution. On the basis of these optimal results, three screw profile models corresponding to the three cases were designed for further numerical simulations in order to evaluate and predict the operating behavior of the high-load screw press. This process is described through a block diagram representing the simulation of sawdust pressing in the screw press–compression chamber system.

The geometric model of the screw press–compression chamber system was designed to include three main components. The feeding hopper 1 is responsible for delivering sawdust uniformly onto the screw shaft, thereby minimizing the risk of clogging. The screw press 2 is designed to generate axial compressive forces acting on the material, increasing its density and forming the briquettes. The compression chamber and outlet die 3 serve to control the material flow, ensuring that the final product achieves a stable shape and consistent dimensions.

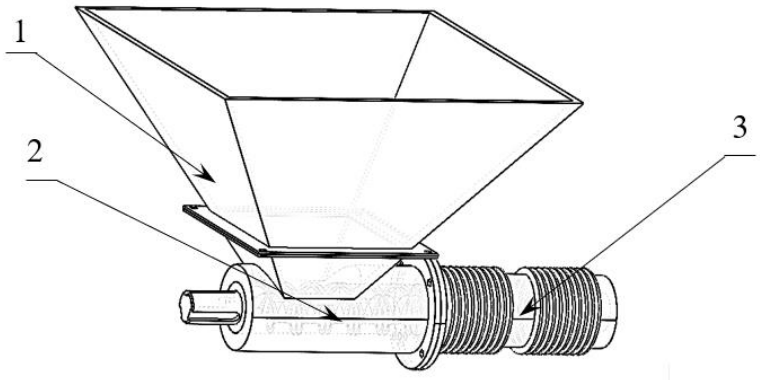

Figure 2: Geometric model of the screw press–compression chamber system

Using the EDEM software, three simulation models were developed to investigate the sawdust pressing process. The first model simulates the pressing process using the screw geometry currently employed in the factory. The second model simulates the process with a screw whose geometry has been modified based on the results of the previous analyses. The third model represents the pressing process using a more highly optimized screw geometry, also derived from analytical results and actual operating conditions. These models form the basis for evaluating and comparing compression capability, force distribution, and wear behavior, thereby identifying the most effective design solution.

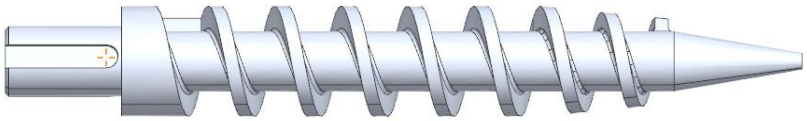

Figure 3: 3D model of the screw press - Model 1

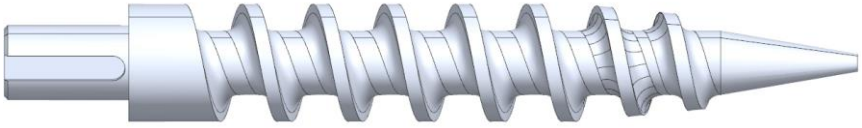

Figure 4: 3D model of the screw press - Model 2

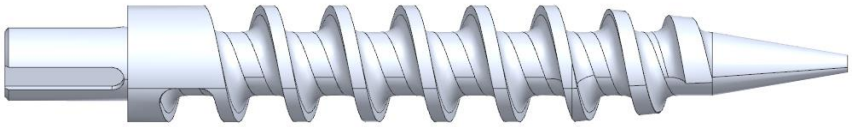

Figure 5: 3D model of the screw press - Model 3

In this study, two types of materials were considered: sawdust and C45 steel. Sawdust particles exhibit irregular shapes and sizes, typically ranging from 0.08 mm to 0.6 mm, and their composition varies depending on wood type and manufacturing process. Due to these characteristics, the Discrete Element Method (DEM) was selected, as it enables detailed description of particle interactions throughout the pressing process. To obtain accurate simulation results, it is necessary to define operating conditions that closely match real conditions, including parameters such as particle size and shape, density, elastic modulus, Poisson's ratio, friction coefficient, cohesive force, and restitution coefficient. These parameters govern the ability to predict flow behavior, compaction level, and wear on the screw surface. In DEM simulations, two common approaches are used: the perfectly rigid model and the relatively rigid model. In this research, the relatively rigid approach was adopted because it allows more detailed representation of particle collisions and wear processes. Particle motion is computed according to Newton's laws, with particle positions and velocities updated at each small time step, enabling accurate reproduction of the system's particle dynamics. The time step is selected based on the Rayleigh time criterion to ensure numerical stability and simulation accuracy. To reduce computational cost, a spatial subdivision algorithm is employed to divide the simulation domain into three-dimensional cells, such that collision detection is performed only between particles within the same or neighboring cells. Once collisions are detected, contact forces are

calculated and used to update particle positions and velocities in the subsequent time step.

The wear of the screw press is determined based on the difference in mass before and after operation or calculated from the measured wear depth. In DEM simulations, particle shape is a critical factor for ensuring accuracy. A simple spherical particle model offers the advantage of low computational cost but cannot adequately represent the irregular geometry and mechanical interlocking mechanisms of real materials. In contrast, polyhedral particle models or highly detailed particle shape descriptions provide higher accuracy but require significantly greater computational effort. Therefore, this study adopts a calibrated representative model that uses clusters of multiple spherical particles to reproduce the irregular geometric characteristics of sawdust while maintaining reasonable computational efficiency. During the simulation process, in addition to the properties of the bulk material, the mechanical characteristics of rigid components such as the screw press and compression chamber made of C45 steel must also be accurately defined. Appropriate boundary conditions play a crucial role, not only in simulating material conveying and compaction but also in predicting force distribution along the screw axis, identifying high-pressure regions, and locating areas prone to wear. After establishing these parameters, the sawdust pressing process was simulated using the EDEM software with a simulation time scaling factor of 1:1. The simulation was conducted over a working duration equivalent to 60 hours, using a very small time step to ensure high accuracy in calculating and tracking interactions between particles and the screw surface. With approximately 60 million computational steps per 60 seconds of simulated time on the computer, the results allow for detailed analysis of force distribution, pressure evolution, and wear generation. The same modeling and simulation setup was applied to the other geometric models of the screw press that were developed. The simulation results from these models were then compared and analyzed to evaluate design effectiveness and identify regions requiring adjustment in order to enhance system performance and durability under real operating conditions.

The simulation results of the three screw press models under the established conditions reveal clear differences in compressive pressure distribution and magnitude. In the first model, pressure increases slowly at the initial stage and then rises rapidly, indicating instability during the early phase of operation. The pressure distribution is highly non-uniform along the screw,

with localized concentration at specific regions, leading to material accumulation, localized blockage, and significant heat generation. The second model exhibits a rapid initial compression stage, followed by relatively stable pressure with small fluctuations. In this case, the pressing process reaches a well-compacted state, with particles effectively rearranged to minimize void spaces. However, the high pressure at the final sections of the screw shaft results in severe wear in these regions. The third model demonstrates a rapid initial compression phase, after which the pressure remains stable at a lower level compared to the other two models. The pressure distribution within the compression chamber is uniform across the entire pressing zone, without forming regions of excessive pressure concentration. This behavior helps reduce wear and limit damage while maintaining stable operating conditions.

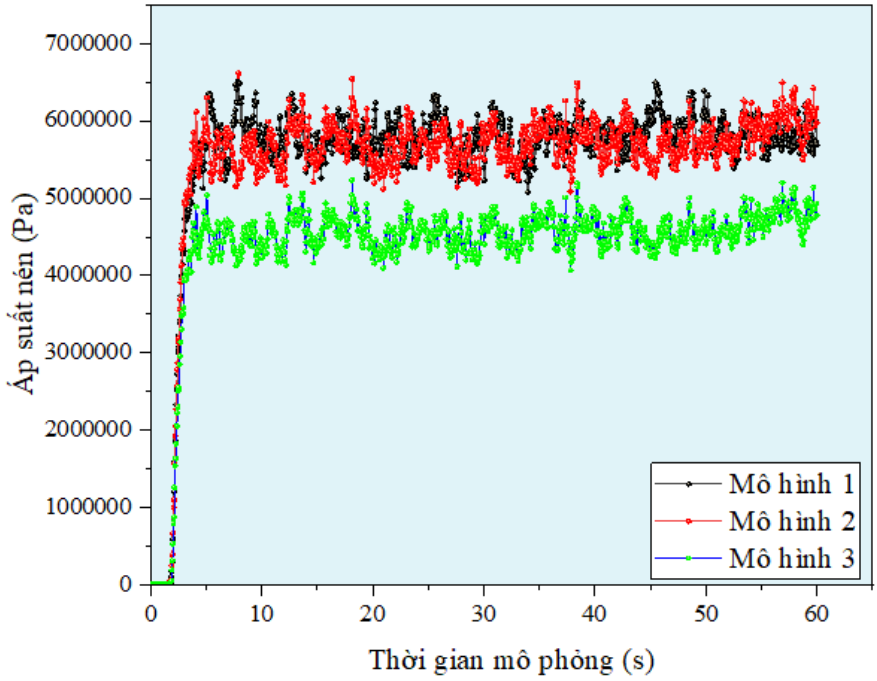

Figure 6: Pressure-time curves for the three models

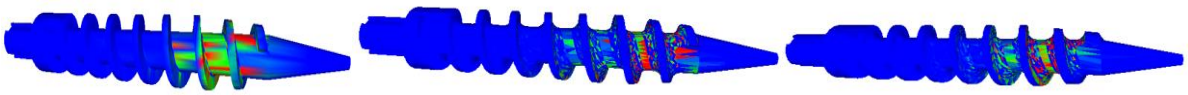

Figure 7: Pressure distribution contours for the 3 models

The compressive force is a key factor that directly affects the operating performance of a screw press, as it represents the total force acting on the material along the screw axis throughout the pressing process. Simulation results show that, in the first model, the compressive force is strongly concentrated in the last three screw flights, with a particularly high increase at

the second flight. The force distribution is highly non-uniform, appears relatively late, and is concentrated near the outlet region, causing the screw to experience large localized stresses. This condition leads to accelerated wear and a high risk of damage at these locations. In the second model, the compressive force appears earlier, is more evenly distributed along the compression zone, and gradually increases toward the end of the screw. This trend is beneficial for enhancing compaction in the final stage, allowing the briquettes to reach maximum density before exiting the compression chamber. However, the sharp increase in compressive force near the outlet causes the screw to be subjected to high loads and stresses, which may result in severe wear and deformation in this region during long-term operation. The third model exhibits a relatively low and stable compressive force over the entire length of the compression zone. This characteristic reduces the mechanical load acting on the screw, limits friction and wear, and contributes to an extended service life of the equipment. Nevertheless, because the compressive force remains at a lower level, the briquettes produced by this model may not achieve the same compactness and density as those obtained from the first two models. From the comparative results, the first and second models ensure high briquette strength but are associated with a higher risk of wear, whereas the third model prioritizes screw durability by maintaining a lower compressive force, albeit at the potential expense of final product quality.

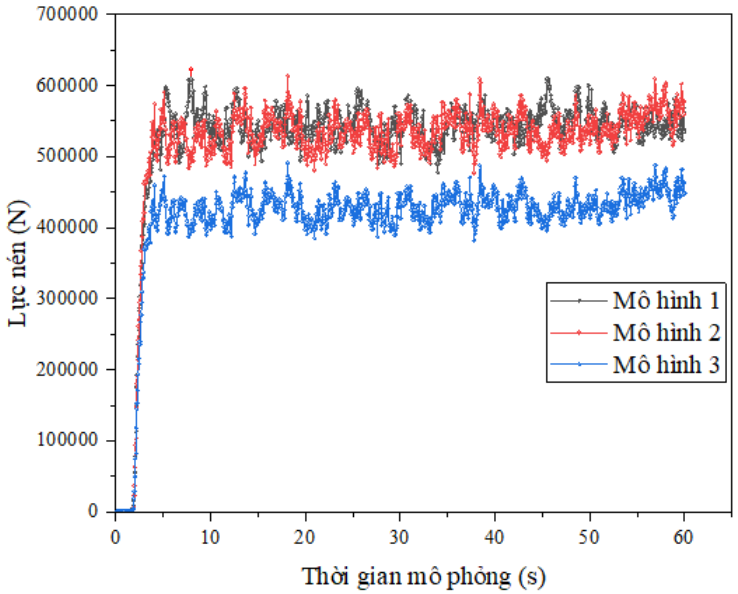

Figure 8: Total compressive force curves of the 3 models

Figure 9: Distribution of total compressive force in the three models

The total force acting on the screw press consists of normal force, tangential force, and friction force, which are mainly concentrated in the bulk material compression zone. Simulation results indicate clear differences in force distribution among the three models. In the first model, the total force is strongly concentrated at the second screw flight and increases significantly toward the outlet region. This high force level ensures strong material compaction, producing briquettes with high density and mechanical strength. However, it also imposes substantial mechanical loads on the screw surface, leading to rapid wear, localized deformation, and a potential risk of cracking in regions subjected to high stresses. In the second model, the total force is slightly lower than that of the first model but remains relatively high overall. The force distribution is more uniform and shows a gradual increase from the inlet to the outlet of the screw. This progressive increase supports a more controlled compaction process, enabling the production of briquettes with more uniform quality while reducing sudden stress concentration. Nevertheless, the final section of the screw still experiences high loads, which may result in significant wear in this region. The third model exhibits a considerably lower total force compared to the other two models and maintains a stable force level along the entire compression zone. There is no sudden force increase near the outlet, which significantly reduces the mechanical load on the screw and limits friction and wear. Although the lower force may reduce the compaction capability of the material, this model offers a clear advantage in extending screw service life and minimizing the risk of damage during operation.

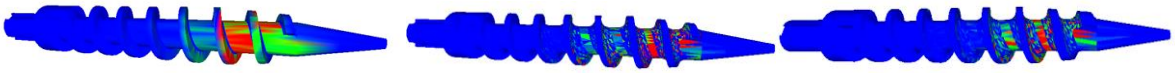

Figure 10: Distribution of total force in the three models

The axial stress of bulk material particles arises when the particles are compressed inside the compression chamber and are subjected to forces transmitted from neighboring particles or from the screw surface. This compressive force is distributed over the cross-sectional area of each particle, generating a certain level of stress. Analysis of the stress distribution in the three models indicates that stress concentration zones are mainly located at the second and third screw flights, where the compressive loads are highest. Simulation results show that the first model maintains the highest axial stress level. This ensures strong material compaction, enhances interparticle bonding,

and produces dense, mechanically robust briquettes; however, it also significantly increases wear on the screw press, particularly in high-load regions. The second model exhibits lower axial stress than the first model, while maintaining a more stable stress distribution with smaller fluctuations. This characteristic reduces the mechanical load acting on the screw compared to the first model, while still ensuring satisfactory briquette compaction quality. The third model shows the lowest axial stress and maintains a stable stress level throughout the simulation. Although this lower stress reduces the compaction degree of the final product, it significantly limits mechanical loading on the screw press, thereby reducing the risk of deformation and wear. Consequently, this model offers a clear advantage in extending the service life of the screw and related mechanical components.

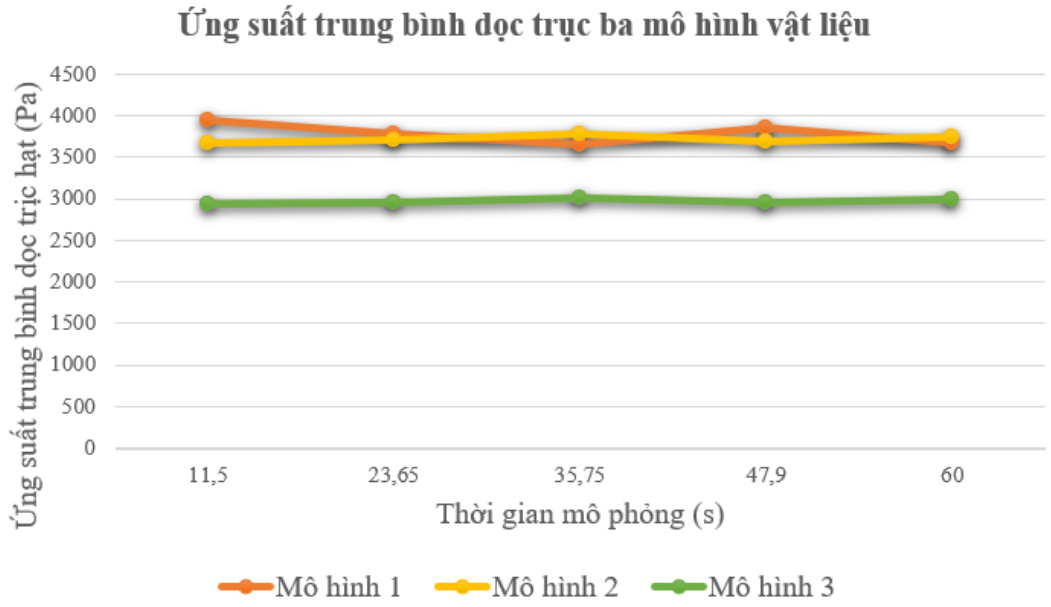

Figure 11: Axial stress curves of the 3 models

The compressive force acting on bulk material during the pressing process originates from contacts between particles and between particles and the screw surface. Simulation results indicate that the average compressive force acting on particles is consistently highest in the first model. This reflects strong compaction capability, enabling the product to achieve high bonding strength and compactness. However, the large compressive force also increases the load acting on the screw press, leading to higher friction and accelerated wear, as well as increased maintenance costs. The second model exhibits an average compressive force only slightly lower than that of the first model. As a result, it still ensures effective compaction of the briquettes while reducing

screw wear to some extent compared to the first model. The third model has the lowest average compressive force and maintains a stable level throughout operation. Although this may result in less compact products, it provides a distinct advantage in reducing the mechanical load on the screw and compression chamber surfaces, limiting friction and wear, extending equipment service life, and lowering maintenance requirements.

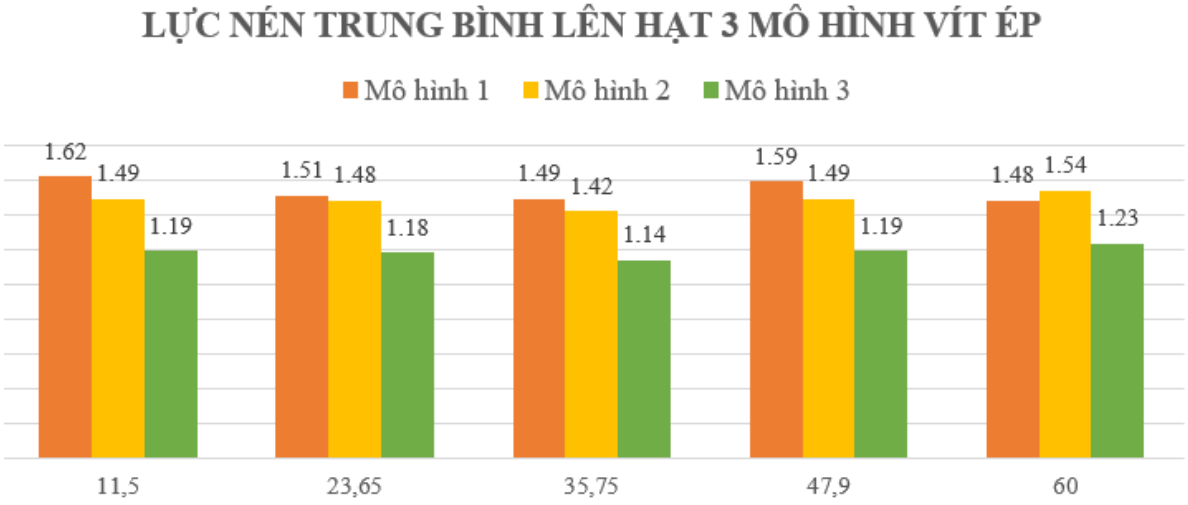

Figure 12: Average compressive force acting on bulk material for the 3 models

The average heat flux is an indicator reflecting the level of heat exchange among particles during the pressing process. A higher heat flux indicates more intense thermal interaction within the particle system, which can promote compaction but also poses a risk of localized overheating. Conversely, a lower heat flux helps limit thermal deformation but may reduce interparticle bonding. Simulation results show that, in all 3 models, heat flux is mainly concentrated in the material compression zone. The first model maintains the highest average heat flux, indicating strong heat generation and transfer within the material system. This enhances compaction and improves briquette bonding; however, it also subjects the screw press to significant thermal loading, increasing the risk of thermal deformation, cracking, and accelerated wear. The second model exhibits a lower average heat flux than the first model, with a more stable thermal distribution. As a result, the risk of thermal deformation of the screw press is reduced while maintaining acceptable compaction performance and briquette quality. The third model shows the lowest and most stable heat flux throughout operation. This significantly reduces thermal effects on the screw, limits deformation, and extends equipment service life. Nevertheless, the lower temperature level may slightly

reduce interparticle bonding, leading to briquettes that are less compact compared to those produced by the other 2 models.

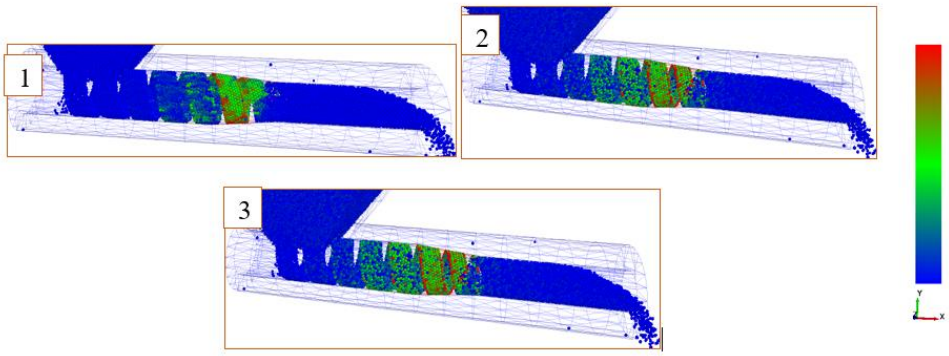

Figure 13: Average heat flux distribution for the 3 models

The average stress tensor on particles reflects the combined stress state within individual particles and across the entire material system during pressing. Simulation results indicate that, in all 3 models, the stress tensor is mainly concentrated at the initial screw flights, particularly the first and second flights, where material compaction is most intense. These regions experience the highest internal forces and directly determine the density and bonding quality of the briquettes. In the first model, the stress tensor consistently remains at the highest level. This enhances compaction capability and produces dense, high-strength briquettes; however, the high stress values also subject the screw press to complex internal loads, increasing the risk of wear, deformation, and cracking at multiple locations, thereby reducing equipment service life. The second model exhibits lower stress tensor values than the first model, with more stable variations. This stability enables better control of the compaction process, ensuring product quality while reducing complex mechanical loading on the screw press. However, because stress levels remain relatively high, the risk of wear in load-bearing regions still exists. The third model shows the lowest stress tensor values among the three models. This indicates reduced internal loading on the screw press, helping to limit wear, minimize deformation, and lower the risk of failure, while also extending continuous operating time without frequent maintenance.

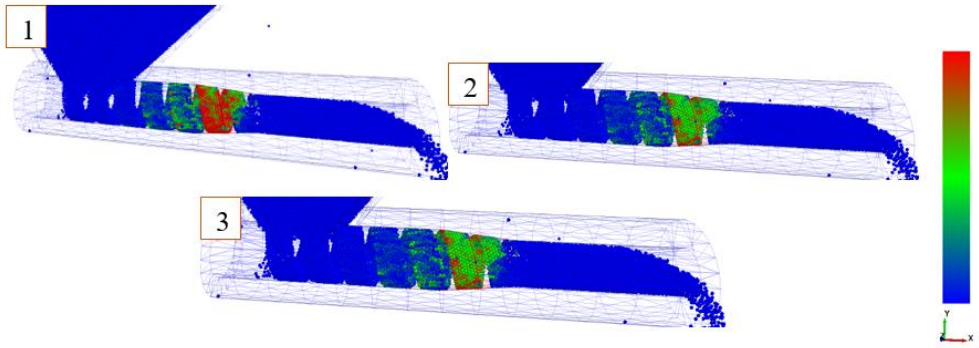

Figure 14: Stress tensor distribution for the three models

The average particle velocity reflects the movement of the material flow during the pressing process and is strongly influenced by the compression conditions at different positions along the screw axis. Simulation results show that higher velocities occur mainly in the feeding zone and at the outlet, where particles move more freely. In contrast, in the highly compacted region, particularly at the second screw flight, the particle velocity decreases significantly due to increased compressive forces that slow down particle motion, thereby increasing density and stabilizing the briquette structure. The calculated results indicate that, in the first model, the average particle velocity is the highest among the three models. This supports rapid feeding and higher throughput, but it also intensifies impacts and friction between particles and the screw surface as well as the compression chamber, leading to accelerated wear. The second model exhibits a lower average particle velocity, with a gradual increase from the inlet to the outlet of the screw. This behavior indicates a more controlled compaction process, limiting sudden impacts and partially reducing wear, although a risk of high friction remains near the outlet region. The third model maintains very low and stable particle velocities throughout the pressing process. This characteristic significantly reduces collisions and friction between particles and the screw surface, thereby lowering wear and extending equipment service life. However, the low velocity may result in reduced productivity and insufficient compaction of the final briquettes unless additional supporting measures are applied.

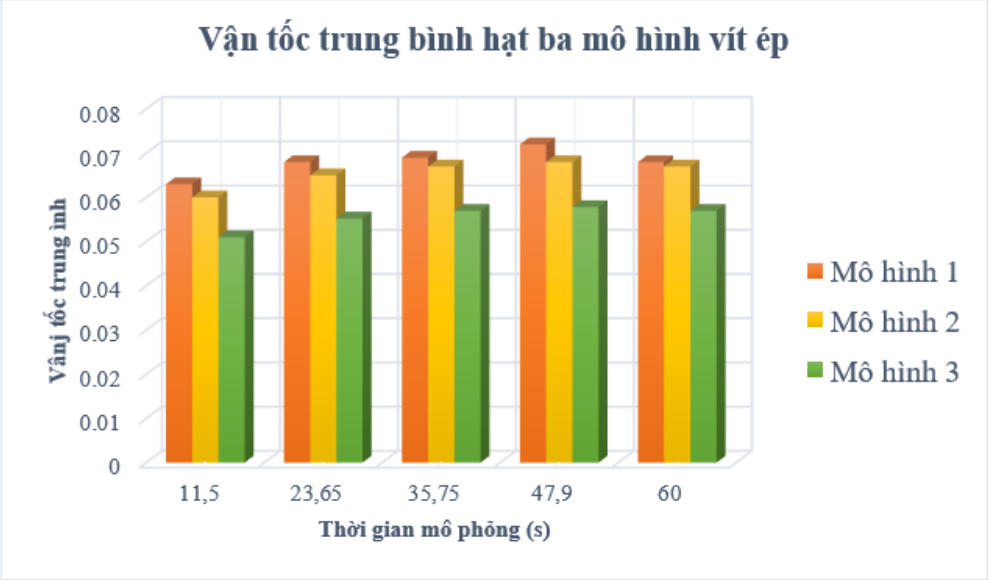

Figure 15: Average particle velocity curves for the 3 models

From the analysis of average particle velocity in the 3 screw press models, it can be observed that velocity not only determines the ability of the particle system to move along the compression chamber but also directly governs the energy state of the material. According to fundamental mechanical theory, the mechanical energy of each particle in DEM simulations consists of two components: kinetic energy, which depends on particle velocity, and potential energy, which depends on particle position in a gravitational field. However, in a screw press operating in a confined space with a horizontally oriented axis, changes in particle position in the gravitational direction are negligible; therefore, potential energy remains nearly constant. In contrast, particle velocity continuously changes due to the action of normal forces, tangential forces, and sliding friction, making kinetic energy the dominant component governing energy transfer within the bulk material system. Consequently, analyzing particle kinetic energy is essential for evaluating the degree of agitation, collision intensity, and energy transmission efficiency of each screw press model.

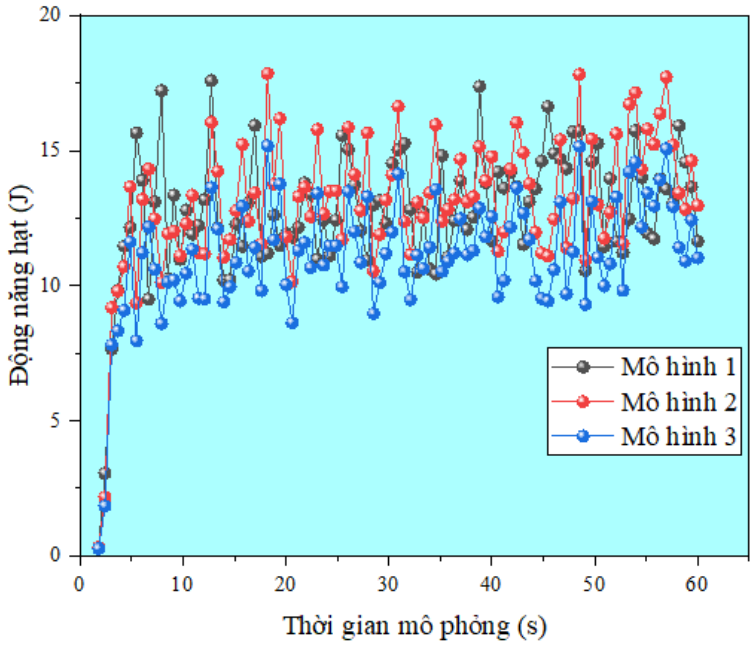

Figure 16: Particle kinetic energy curves for the three models

Wear is the material loss occurring on the surface of the screw press due to the combined effects of friction, mechanical loading, particle impacts, and harsh operating conditions. Simulation results indicate that the first screw press model exhibits the highest wear level, with wear concentrated mainly on the first three screw flights, particularly at the flight roots. The wear rate increases rapidly over time, reaching an average wear depth of 0.0687 mm and a total wear amount of 497.8 mm after 60 hours of simulation. The wear distribution is highly non-uniform and locally concentrated, posing a high risk of premature failure. The second screw press model shows a significant reduction in wear compared to the first model. Wear still primarily occurs on the initial screw flights, but it is more evenly distributed. After 60 hours of simulation, the average wear depth reaches 0.0254 mm, with a total wear amount of 163.2 mm. The geometric modifications applied in this model reduce compressive pressure and improve force distribution, thereby lowering wear and enabling more stable operation. The third screw press model demonstrates superior wear reduction performance. Wear is uniformly distributed over the first three screw flights and is significantly reduced at critical locations. The average wear depth is only 0.0058 mm, while the total wear amount reaches 40.6 mm after 60 hours of simulation. These results clearly demonstrate that optimized geometric design effectively reduces mechanical loading, limits friction, and provides better protection of the screw surface compared to the other 2 models. From an overall comparison, the first

model experiences the highest wear due to high pressure and force levels, which lead to increased friction and heat generation. The second model improves force distribution and reduces wear but still presents a risk of stress concentration at certain locations. The third model achieves the lowest and most stable wear level, significantly extending the service life of the screw press, although additional measures may be required to maintain briquette quality when operating under lower force and pressure conditions.

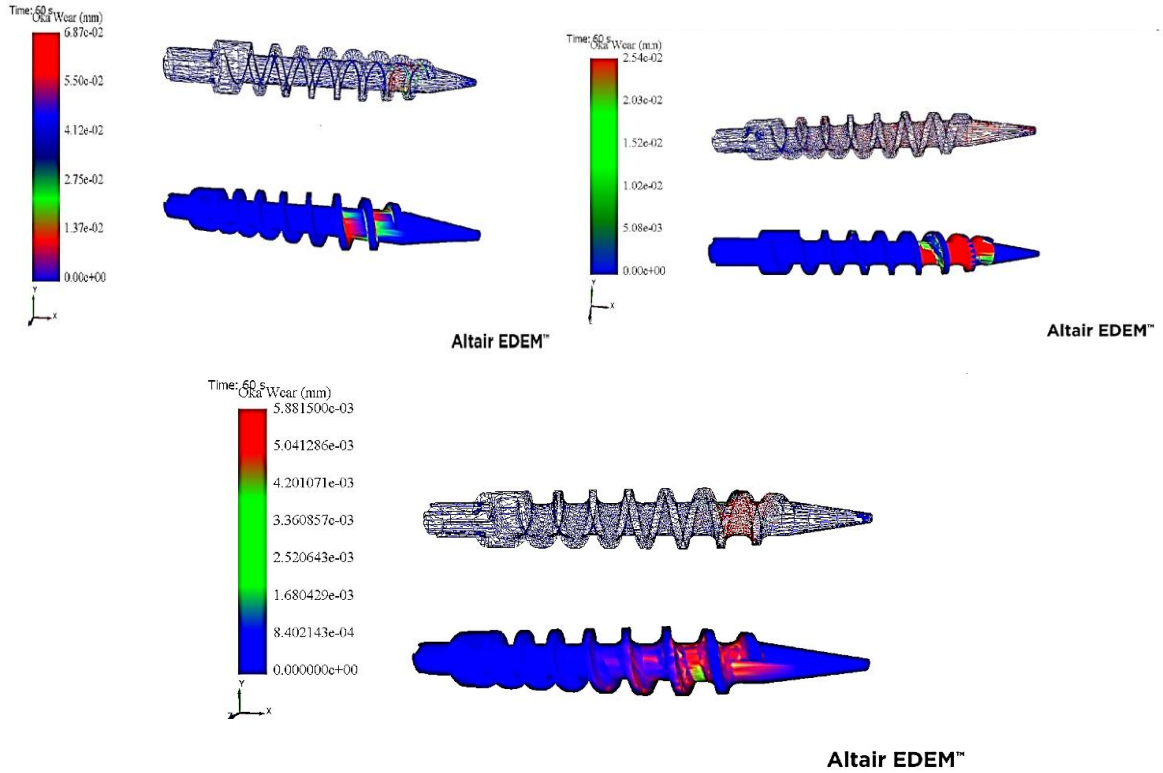

Figure 17: Average wear depth of the three models

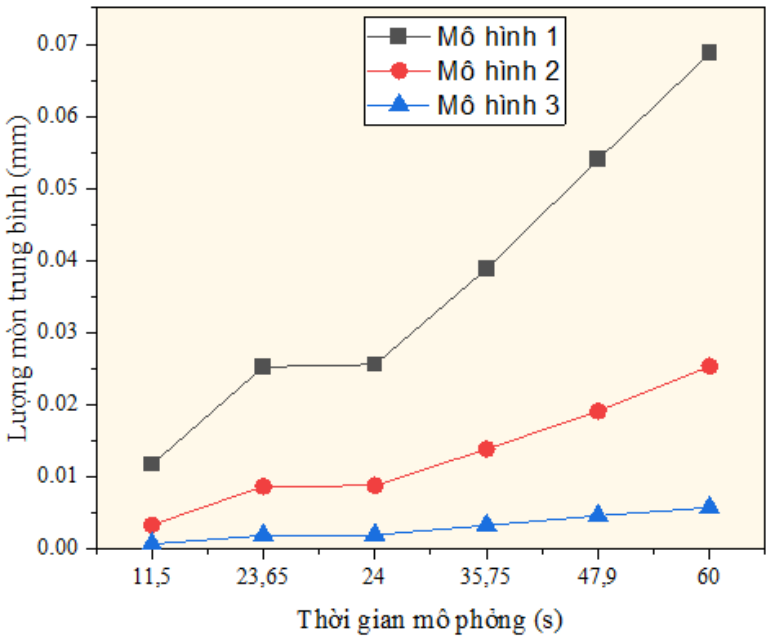

Figure 18: Total wear amount of the 3 models

The results presented in Chapter 2 confirm that the screw press-compression chamber system for sawdust has been successfully established in terms of block diagram representation, geometric modeling, and numerical simulation. Simulation outcomes show that the first and second models achieve high pressure, compressive force, and axial stress, resulting in dense and mechanically robust briquettes. However, these conditions also lead to large total wear amounts, concentrated mainly near the end of the screw shaft, thereby increasing the risk of failure and maintenance costs. In contrast, the third model maintains mechanical indicators at lower and more stable levels, with reduced particle velocity, fewer impacts and frictional interactions, effective wear control, and a more uniform wear distribution along the screw length. Based on the obtained results, it can be concluded that the third model represents the optimal solution, simultaneously satisfying the objectives of wear resistance improvement, maintenance of pressing performance, and enhancement of the operational durability of the screw press. The geometric parameters of Model 3 are presented in Table 1.

Table 1. Geometric Parameters of Screw Press Model 3

No	a_1	a_2	**R_1 (mm)**	**R_2 (mm)**	**h (mm)**	**S_1 (mm)**	**S_2 (mm)**	**e_1 (mm)**	**e_2 (mm)**	**e_3 (mm)**	**e_4 (mm)**
Screw Press Model 3	99°	93°	10	10	12	40	39,5	15	12	9,8	8,5

CHAPTER 3: MATERIALS, EQUIPMENT, AND EXPERIMENTAL INVESTIGATION OF HVOF COATING FORMATION

Chapter 3 presents the fundamental factors governing the wear resistance of coatings, together with the research methodology and experimental evaluation procedures. Wear resistance does not depend on a single parameter but is the combined result of multiple physical and mechanical characteristics, such as coating microstructure, hardness, and coating thickness. These factors interact with one another and collectively influence the ability of the coating to protect the surface against wear. In this context, high-velocity oxygen fuel (HVOF) thermal spraying technology enables precise control of influential parameters, thereby producing coatings with high and stable wear resistance. The experimental methodology was developed to comprehensively evaluate coating wear resistance, and the research steps are illustrated through a block diagram of the experimental procedure.

The substrate material used for manufacturing the screw press and experimental specimens is C45 steel, a widely used material in mechanical engineering that is particularly suitable for helical screw components due to its favorable mechanical properties. Experimental samples were cut directly from the screw press to preserve the actual working geometry and were subsequently surface-coated using HVOF technology. Prior to scanning electron microscopy (SEM) observation and hardness testing, the samples were ground, polished, and etched to ensure adequate surface quality for analysis. The coating material employed consisted of a nickel-based alloy powder reinforced with tungsten carbide (WC).

The HVOF spraying system used in this study was the HP-2700M, which includes a PF-3350 powder feeder with precise flow-rate control, a gas supply system consisting of oxygen, propane, nitrogen, and compressed air, and an MP-2100 flow control unit. The HP-2700M spray gun was selected to ensure appropriate spraying conditions matched to particle size and material properties, thereby enabling effective control of the coating formation process. During the experimental investigation, various measurement instruments were employed to characterize coating properties. A Leica DM750 M optical microscope was used to analyze particle size and coating microstructure at different magnifications, in combination with LAS V4.12 image analysis software. Coating hardness was measured using an ISOSCAN HV2 AC hardness tester, applying Vickers or Knoop diamond indentation methods, with

adjustable loads and precise three-axis positioning. All experiments were conducted at the laboratory of the Faculty of Automotive Mechanical Engineering, Hanoi University of Industry, ensuring high measurement accuracy.

In this study, coating microstructural characterization focused on two key factors: particle size and porosity, both of which have a significant influence on the wear resistance of HVOF-sprayed coatings. The spraying powder used was a nickel alloy reinforced with tungsten carbide (WC), known for its excellent friction resistance and wear resistance, making it suitable for protecting screw presses operating under severe pressure and temperature conditions. The HVOF spraying process was carried out using key parameters including powder feed rate, spraying distance, and oxygen-to-propane ratio. To ensure coating quality, optimal parameters were selected as follows: powder feed rate of 25-35 g/min, spraying distance of 0.2-0.3 m, and an oxygen/propane ratio ranging from 3 to 5. Particle size of the coating was measured using the Leica optical microscope at a magnification of x300. The results indicate that the particle size after HVOF spraying ranged from 401 nm to 2.78 µm. The presence of fine and uniformly distributed particles confirms the high quality of the coating, resulting in a dense surface structure that contributes to improved wear resistance. Coating porosity was also evaluated using SEM images at a magnification of x300, combined with quantitative analysis of porosity percentage. The results show that when appropriate spraying parameters are selected, the coating structure exhibits good density with minimized porosity. This significantly enhances the protective capability of the coating surface under harsh operating conditions of the screw press.

Table 2. Taguchi L9 array with measured porosity values

No	**F (g/min)**	**D (m)**	**R**	**Po (%) (1^{st})**	**Po (%) (2^{nd})**	**Po (%) (3^{rd})**	$\overline{\text{Po}}$ **(%)**
1	25	0.2	4	5.249	5.152	5.373	5.258
2	25	0.25	5	4.973	4.863	4.845	4.894
3	25	0.3	6	3.228	3.348	3.148	3.241
4	30	0.2	5	5.059	4.943	4.875	4.959
5	30	0.25	6	3.086	3.294	3.102	3.161
6	30	0.3	4	3.986	4.034	3.883	3.968
7	35	0.2	6	4.688	4.832	4.593	4.704
8	35	0.25	4	3.767	3.912	3.871	3.850
9	35	0.3	5	3.109	3.135	3.285	3.176

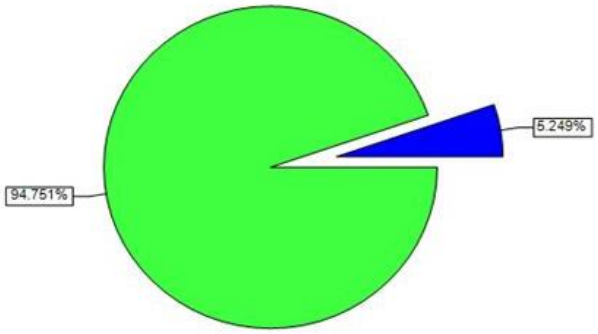

Figure 19: Percentage-based analysis image of coating porosity

Coating hardness is a key factor determining wear resistance. During the coating formation process, sprayed particles impact the surface at high velocity, causing plastic deformation and peening of the material, which increases coating density and hardness. In particular, HVOF spraying technology, characterized by high particle velocities and relatively lower heat source temperatures, enhances coating strength and hardness compared to other thermal spraying methods. In this study, experimental specimens were produced under 9 different spraying conditions to investigate the influence of spraying parameters on coating hardness. Three parameters were varied at 3 levels each: powder feed rate at 25, 30, and 35 g/min; spraying distance at 0.2, 0.25, and 0.3 m; and oxygen-to-propane ratio at 4, 5, and 6. The hardness values measured for samples produced under the 9 spraying conditions are summarized in the Taguchi L9 orthogonal array. The results reveal a clear variation in coating hardness depending on the combination of spraying parameters.

Table 3. Taguchi L9 array with measured hardness values

No	**F (g/min)**	**D (m)**	**R**	**H (HRC) (1st)**	**H (HRC) (2nd)**	**H (HRC) (3rd)**	**$\overline{H}$ (HRC)**
1	25	0.2	4	70.51	71.07	70.92	70.83
2	25	0.25	5	75.76	74.70	73.96	74.81
3	25	0.3	6	70.03	69.29	69.12	69.48
4	30	0.2	5	71.30	70.66	69.72	70.56
5	30	0.25	6	72.45	71.87	72.98	72.43
6	30	0.3	4	76.44	75.85	75.19	75.83
7	35	0.2	6	70.78	71.21	71.73	71.24
8	35	0.25	4	78.67	79.3	76.50	78.16

9	35	0.3	5	71.57	70.22	71.28	71.02

The coating thickness on the C45 steel substrate was determined using a Leica optical microscope at a magnification of x300, allowing accurate observation and measurement of the coating structure after HVOF spraying. Measurements from nine experimental samples show that the coating thickness ranges from 406.518 µm to 747.009 µm. This range reflects the stability of the spraying process and demonstrates effective control of spraying parameters to produce coatings with high thickness uniformity. The results also confirm that the HVOF method not only provides strong coating adhesion but also ensures sufficient thickness, thereby contributing to extended service life and improved operational performance of coated mechanical components.

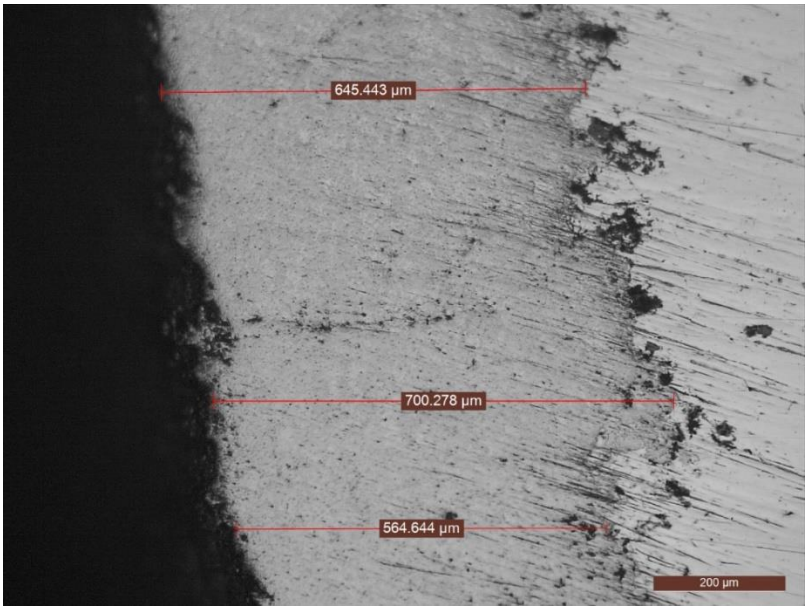

Figure 20: x300 magnification image used to measure coating particle size

In this study, HVOF spraying powders composed of WC and Ni were selected due to their excellent resistance to wear, high temperature, and high pressure, making them suitable for producing wear- and corrosion-resistant coatings. The powders were mixed at different ratios for spraying, mechanical property measurement, and practical testing. Experimental results indicate that the resulting coatings exhibit fine particle sizes (0.4-2.8 µm), low porosity, and high hardness. HVOF-sprayed coatings form dense, thick layers (400-750 µm). Microstructural analysis reveals a lamellar structure characterized by stacked metallic splats. Thickness measurements obtained using the Leica optical microscope confirm coating thicknesses in the range of 400-750 µm, which are sufficient to protect the surface without inducing excessive residual stresses. A Taguchi experimental design was developed to evaluate the microstructure and hardness of HVOF coatings, enabling the identification of optimal processing parameters that yield the best

coating structure and hardness. These characteristics are decisive factors governing coating wear resistance. The wear resistance of the screw press will be further tested and evaluated through practical operation of the screw press under real working conditions.

CHAPTER 4: EXPERIMENTAL TESTING AND EVALUATION OF THE WEAR RESISTANCE OF HIGH-LOAD SCREW PRESSES

Chapter 4 focuses on experimental investigations and result analysis to evaluate the wear resistance of high-load screw presses under real operating conditions.

The experimental procedure and evaluation of wear resistance under actual working conditions are presented in this chapter. The experiments were conducted by comparing the wear amounts of 4 types of screws: screw press Model 1, screw press Model 1 with HVOF coating, optimized screw press (Model 3) without coating, and optimized screw press with HVOF coating. Each screw was installed in the same pressing machine and operated continuously for 24 hours under identical working conditions and operating parameters. After testing, the screws were accurately weighed to determine mass loss due to wear. The results show that the uncoated factory screw exhibits the highest average wear, reaching 94.44 g, whereas the factory screw with HVOF coating shows a significantly reduced wear of 43.33 g, corresponding to a reduction of 52.2%. Similarly, improvements in screw geometry alone demonstrate a clear effect: the optimized uncoated screw exhibits a reduced wear of 70 g compared to 94.44 g for the original design. When combined with HVOF coating, the optimized screw achieves the lowest wear level of only 28.89 g, representing a reduction of 58.2% compared to the uncoated optimized screw. These results confirm that both geometric optimization of the screw design and the application of HVOF coating play critical roles in enhancing the wear resistance of high-load screw presses. Notably, the combination of both solutions provides the most effective improvement, significantly extending service life, reducing maintenance costs, and enhancing the operational efficiency of high-load screw press systems.

After completing the wear measurements using the mass-loss method, 3D scanning technology was employed to perform a more detailed inspection of the distribution, morphology, and degree of localized wear on the screw press surface. Statistical analysis of geometric deviations for the three screw press models reveals clear differences in wear severity and surface stability. Model 1 exhibits the largest negative deviation (-2.613 mm) and the highest mean negative deviation (-0.3991 mm), indicating severe and non-uniform surface wear. In addition, the standard deviation (1.8446) and variance (2.7046) are relatively high, reflecting a wide dispersion of errors and significant instability during operation. In Model 2, although the mean deviation (-0.3302

mm) and average wear level (-1.5065 mm) show some improvement compared to Model 1, the overall root-mean-square (RMS) deviation (2.0766) and variance (3.0914) are higher. This suggests that, despite a moderate average deviation, errors are unevenly distributed, with the presence of localized surface defects. The standard deviation of this model (1.6227) remains relatively high, indicating insufficient stability for high-precision engineering applications. In contrast, Model 3 demonstrates superior geometric quality, with a small mean deviation (-0.2263 mm), an RMS value of only 0.8523, a standard deviation of 0.8518, and a variance of just 0.7256 - the lowest among the 3 models. These results indicate that geometric deviations are well controlled and uniformly distributed over the entire surface. Notably, the mean negative deviation is only -0.2333 mm, reflecting a low wear level and minimal material loss. Overall, these findings confirm that Model 3 is the optimal choice in terms of geometric accuracy, wear resistance, and surface stability, outperforming the other two models and offering greater reliability for industrial production.

The comparison results between the CAD design model and the 3D scanning data obtained from the actual manufactured product show that the geometric deviations remain within allowable limits and are fully consistent with the previously calculated results. This confirms that the design approach, geometric calculations, and selection of initial parameters are appropriate, ensuring both dimensional accuracy and manufacturability.

In conclusion, this research has focused on optimizing the design of high-load screw presses and applying HVOF coating technology to improve wear resistance. Analytical and experimental investigations demonstrate that adjusting the screw profile - particularly increasing the flight thickness in load-bearing regions - helps to achieve a more uniform force distribution and reduces localized wear. The third screw press model, featuring an optimized design combined with HVOF coating, exhibits superior load-bearing capacity, reduced deformation, and stable geometric integrity during operation. Simulation results further confirm that wear is primarily concentrated in the region spanning the first to the third screw flights; however, the wear level decreases progressively from Model 1 to Model 3, significantly extending service life.

HVOF coating technology has proven effective in producing high-quality protective layers. The coatings exhibit a lamellar structure with thicknesses ranging from 400 µm to 750 µm, as verified by optical microscopy. The key

factors influencing coating properties were clearly identified: spraying distance has the greatest effect on porosity and hardness, while the oxygen-to-propane ratio primarily governs coating adhesion. Based on experimental data, regression-based mathematical models were developed, enabling the determination of optimal spraying parameters to enhance coating performance.

For future research, further investigation of alternative coating materials and optimization of HVOF parameters is recommended to continue improving wear resistance while reducing costs. Advanced coating solutions, such as composite coatings or high-temperature-resistant coatings, should be explored to enhance surface protection. In parallel, the application of artificial intelligence techniques in simulation and design optimization is expected to improve the accuracy of wear and service life prediction. Moreover, extending experimental validation across diverse production environments will allow for a more comprehensive assessment of varying operating conditions. Finally, the development of intelligent screw press designs incorporating sensors, along with the exploration of environmentally friendly bio-based coatings, represents a promising research direction that addresses both technical performance and environmental sustainability requirements.

LIST OF PUBLICATIONS

[1]. **Hong Tien Nguyen**, Tuan-Linh Nguyen, Nguyen Van Thien, Phan Van Quoc "*Enhancement of Wear Resistance of High-Load Pressing Screw in Smokeless Charcoal Production by Using Genetic Algorithm and Discrete Element Method*", Tribology in Industry (Q3 Scopus), Vol. 46, No. 1 (2024) 151-162, DOI: 10.24874/ti.1568.11.23.01.

[2]. Tuan-Linh Nguyen, **Nguyen Hong Tien**, Van Thien Nguyen, Duc Duong Khuat, "*Analysis of the effect of spray mode on coating porosity and hardness when spraying press screws by the high velocity oxy fuel method*", EUREKA Physics and Engineering (Q3 Scopus), November 2023, DOI: 10.21303/2461-4262.2023.003161.

[3]. **Hong Tien Nguyen**, Tuan Linh Nguyen, Van Thien Nguyen, Long Hoang**,** *"Investigation of the Impact of HVOF Spraying Parameters on the Abrasion Resistance of Tungsten Carbide Coatings"*, Engineering, Technology & Applied Science Research (Q2 Scopus), Volume: 14 | Issue: 6 | Pages: 17769-17773 |December2024, https://doi.org/10.48084/etasr.7996

[4]. **Chủ nhiệm đề tài cấp cơ sở:** "*Nghiên cứu giải pháp mô phỏng nhằm đánh giá tình trạng mòn của vít ép mùn cưa ứng dụng tại nhà máy sản xuất than sạch*", Đề tài nghiên cứu khoa học năm 2023 đã bảo vệ thành công. Hội đồng nghiệm thu đánh giá đạt.

[5]. **Thư ký khoa học:** "*Nghiên cứu ứng dụng công nghệ tạo lớp phủ Cermet bằng phương pháp HVOF để nâng cao tuổi thọ vít ép của máy ép trong công nghiệp chế tạo than sạch*", Đề tài Sở khoa học và Công nghệ Thành phố Hà Nội năm 2022 đã bảo vệ thành công tháng 06 năm 2025. Hội đồng nghiệm thu đánh giá đạt.

REFERENCES

Vietnamese

[1] Đề tài, mã số KC 05.10, *Nghiên cứu xác định độ chịu mài mòn và độ bám dính lớp phủ bột hợp kim ZRO-182 trên nền vật liệu nimonic 263 (được sử dụng chế tạo ống vòi voi trong các nhà máy nhiệt điện) có lớp phủ trung gian bột hợp kim NiCrAlY*.

[2] Đề tài, mã số: 01C-01/04-2009-2, *Nghiên cứu ảnh hưởng của khoảng cách phun, vận tốc phun, lưu lượng phun đến độ xốp, độ bám dính lớp phủ bột hợp kim Cr20Ni3 trên nền trục thép 40Cr bằng phương pháp phun nổ*.

[3] Lê Thu Quý (2004), *Khảo sát công nghệ tạo lớp phun phủ giả hợp kim Zn-Al trên nền thép CT3 và khả năng bảo vệ chống ăn mòn của lớp phủ này*. Đề tài khoa học, Viện Kỹ thuật nhiệt đới - Viện hàn lâm KH&CN Việt Nam.

[4] Lê Thu Quý (2007), *Nghiên cứu ảnh hưởng của các yếu tố môi trường khí quyển Hà Nội tới tốc độ ăn mòn của lớp phun phủ kẽm chế tạo tại Viện Kỹ thuật nhiệt đới*. Đề tài khoa học, Viện Kỹ thuật nhiệt đới - Viện hàn lâm KH&CN Việt Nam.

[5] Lê Thu Quý (2012), *Nghiên cứu chế tạo lớp phủ hợp kim niken crôm bằng công nghệ phun phủ hồ quang điện để bảo vệ chống ăn mòn cho các chi tiết máy bơm công nghiệp làm việc trong môi trường axít*. Đề tài khoa học, Viện Kỹ thuật nhiệt đới - Viện hàn lâm KH&CN Việt Nam.

[6] Nguyễn Chí Bảo (2016), *Nghiên cứu ảnh hưởng của lưu lượng và tốc độ chuyển động tương đối giữa đầu phun với chi tiết đến chất lượng bề mặt phun phủ bằng công nghệ phun nhiệt khí tốc độ cao – HVOF*, LATS, Đại học Mỏ địa chất.

[7] Nguyễn Thanh Phú (2019), *Nghiên cứu ảnh hưởng của một số thông số công nghệ phun phủ HVOF đến chất lượng lớp phủ bề mặt chi tiết làm việc trong điều kiện khắc nghiệt bị mòn*, LATS, Viện Nghiên cứu cơ khí.

[8] Nguyễn Tuấn Linh, Nguyễn Văn Tuân, & Hoàng Xuân Khoa. (2018). *Nghiên cứu tối ưu hóa biên dạng vít ép trong máy ép mùn cưa phục vụ sản xuất than không khói*. Tạp chí Khoa học và Công nghệ, 56, 123–130.

[9] Nguyễn Văn Thảo, & Nguyễn Văn Vượng. (2018). *Ảnh hưởng của cấu trúc vít đến hiệu quả ép và phân bố áp lực trong vít tải trọng cao*. Tạp chí Khoa học và Công nghệ, 56, 45–50.

[10] Phạm Văn Liệu (2016), *Nghiên cứu ảnh hưởng của một số thông số công nghệ đến chất lượng phục hồi bề mặt trục có hình dáng phức tạp bị mòn bằng công nghệ phun phủ*. Luận án tiến sĩ kỹ thuật – Đại Mỏ địa chất, Hà nội.

English

[11]] A. Hassanpour and M. Pasha, *"Discrete element method applications in process engineering"* in CRC Press eBooks, 2019, pp. 333–370. doi:

10.1201/9780429451010-9.

[12] A.G. Lekatou, D. Sioulas, D. Grimanelis (2023), *Corrosion and wear of coatings fabricated by HVOF-spraying of nanostructured and conventional WC-10Co-4Cr powders on Al7075-T6*. International Journal of Refractory Metals and Hard Materials. Volume 112, April 2023, 106164. https://doi.org/10.1016/j.ijrmhm.2023.106164

[13] Aca Jovanovic (2015). *Discrete element modelling of screw conveyor-mixers*. Journal of Chemical Industry, 2015 Volume 69, Issue 1, Pages: 95-101.

[14] Andrew Grima (2013). *Predicting bulk flow and behaviour for design and operation of handling and processing plants*. 11th International Congress on Bulk Materials Storage, Handling and Transportation, Newcastle, Australia, 2013, pp.1-10.

[15] Cundall, P. A. (1971). *A Computer Model for Simulating Progressive Large Scale Movements in Blocky Rock Systems*, In International Society for Rock Mechanics (Eds.), Proceedings of the Symposium of the International Society of Rock Mechanics (pp. 2-8). Rubrecht.

[16] Cundall, P. A., & Strack, O. D. L. (1979). *A discrete numerical model for granular assemblies*. Géotechnique, 29(1), 47–65.

[17] D. Kretz, S. Callau-Monje, M. Hitschler, A. Hien, M. Raedle, J. Hesser (2015). *Discrete element method (DEM) simulation and validation of a screw feeder system*. Powder Technology, 278, 248–256.

[18] Deb, K., Pratap, A., Agarwal, S., & Meyarivan, T. (2002). *A fast and elitist multiobjective genetic algorithm: NSGA-II*. IEEE Transactions on Evolutionary Computation, 6(2), 182–197.

[19] Dellinger, J. G., et al. (2016). *Optimization of screw design for continuous wet granulation: A case study of metoprolol succinate ER tablets*. International Journal of Pharmaceutics, 511, 334–345.

[20] EDEM. (2020). *EDEM-Modelling wear in EDEM and ebook What_is DEM theoretical background behind the Discrete Element_Method*. Altair Engineering Inc.

[21] Ewa Jonda (2024), *Microstructure, residual stress and mechanical properties of double carbides cermet coatings manufactured on AZ31 substrate by high velocity oxy-fuel spraying*. Archives of Civil and Mechanical Engineering, Volume 24, article number 61, (2024).

[22] Ewa Jonda, Leszek Łatka, Artur Maciej, Alexandr Khozhanov (2023) *Investigations on the Microstructure and Corrosion Performance of Different WC-based Cermet Coatings Deposited by High Velocity Oxy Fuel Process onto Magnesium Alloy Substrate*. Advances in Science and Technology Research Journal 2023, 17(2), 25–35.

https://doi.org/10.12913/22998624/160513

[23] F. Schramm, et al. (2020). *Modelling of abrasive material loss at soil tillage via scratch test with the discrete element method*. Journal of Terramechanics 91 (2020) 275–283.

[24] Gaspar-Cunha, A., et al. (2020). *Optimization of single screw extrusion*. International Polymer Processing, 26(4), 417–428.

[25] Giovanni Bolelli, Lutz-Michael Berger, Matteo Bonetti, Luca Lusvarghi. *Comparative study of the dry sliding wear behaviour of HVOF-sprayed WC-(WCr)2C-Ni and WC-CoCr hardmetal coatings*. Wear, Volume 309, Issues 1–2, 15 January 2014, Pages 96-111.https://doi.org/10.1016/j.wear.2013.11.001

[26] J. F. Archard, "*Contact and rubbing of flat surfaces*," Journal of Applied Physics, vol. 24, no. 8, pp. 981–988, Aug. 1953, doi:10.1063/1.1721448.

[27] J. Pulsford (2018), *Effect of Particle and Carbide Grain Sizes on a HVOAF WC-Co-Cr Coating for the Future Application on Internal Surfaces: Microstructure and Wear*. Journal of Thermal Spray Technology, Volume 27, pages 207–219, (2018). https://link.springer.com/article/10.1007/s11666-017-0669-8

[28] J. Pulsford (2019), *Application of HVOF WC-Co-Cr coatings on the internal surface of small cylinders: Effect of internal diameter on the wear resistance*, Wear, Volumes 432–433, 15 August 2019, 202965. https://doi.org/10.1016/j.wear.2019.202965

[29] Jin, Y., Olhofer, M., & Sendhoff, B. (2017). *A framework for evolutionary optimization with approximate fitness functions*. IEEE Transactions on Evolutionary Computation, 6(5), 481–494.

[30] Kretz, T. (2016), *Simulation of the conveying behavior of granular material in a single screw feeder using Blender*. Computer Physics Communications, 200, 25–32.

[31] M. Kremmer, "*A discrete element method for industrial granular flow applications*," Ph.D. dissertation, Dept. Agricultural & Environmental Science, Newcastle Univ, Newcastle upon Tyne, UK, 2001.

[32] M.P. Alekxandrop, *Podgiemno-transportnue masinu, Masinostroenhie*, Maskova, 1984.

[33] Matúš, M., Macek, J., & Macků, L. (2011). *Analysis of tool geometry for screw extrusion machines*. Chemické Listy, 105, 228–231.

[34] Mitchell, Melanie (1975). *An Introduction to Genetic Algorithms*. Cambridge, MA: MIT Press. ISBN 9780585030944

[35] Montgomery, D. C., & Runger, G. C. (2010), *Applied Statistics and Probability for Engineers*. John Wiley & Sons.

[36] Muhammad Firdaus (2017), *Preliminary Design on Screw Press Model of*

Palm Oil Extraction Machine. Materials Science and Engineering, 165 (2017), doi:10.1088/1757-899X/165/1/012029

[37] Nazerke Muratzhankyzy (2021), *Design and engineering calculation of a screw press for extracting juice from sea buckthorn*. Journal of Engineering and Applied Sciences, Vol. 16, no. 8, april 2021

[38] Pawlowski L (2008), *The Science and Engineering of Thermal Spray Coatings*. India, Wiley

[39] Perazzo, P., et al. (2019), *Numerical modeling of the pattern and wear rate on a structural steel plate using DEM*. Mining Engineering, 134, 88–96.

[40] Peter Krizan (2013). *Relationship between technological and material parameters during densification of beech sawdust*. Biomass and Bioenergy, 59, 71–78.

[41] Pétrowski, Alain; Ben-Hamida, Sana (2017). *Evolutionary algorithms*. John Wiley & Sons. p. 30. ISBN 978-1-119-13638-5.

[42] Pezo (2018), *Discrete element model of particle transport and premixing action in a single screw feeder*. Powder Technology, 329, 12–24.

[43] Pezo, L., et al. (2019). *Discrete element model of particle transport and premixing action in modified screw conveyors*. Powder Technology, 329, 12–24.

[44] Potente, H., & Thümen, H. (2006), *Optimization of screw elements in twin-screw extruders*. Polymer Engineering & Science, 46(10), 1342–1350.

[45] R. A. K. Editor-In-Chief, "*Materials handling handbook*," in Wiley eBooks, 1985. doi: 10.1002/9780470172490.

[46] Radjai, F., & Dubois, F (2014), *In Discrete Element Method to Model Grain Flow and Particle Systems*. Springer. Discrete element method applications in process engineering

[47] Rajakumar, S., & Kumar, V. (2013), *Optimization of process parameters using genetic algorithm for friction stir welding of cast aluminium alloy*. Transactions of Nonferrous Metals Society of China, 23(2), 293–301.

[48] Rorres, C. (2000), *The turn of the screw: Optimal design of an Archimedes screw*. Journal of Hydraulic Engineering, 126(1), 72–80.

[49] Roy, R. K. (2001), *Design of experiments using the Taguchi approach: 16 steps to product and process improvement*. Wiley-Interscience.

[50] Sagar (2016), *A Review on Thermal Spray Coating Processes*. International Journal of Trend in Research and Development, 2, 556–563.

[51] Shuai Cao, Zhiyong Chang, Shuofan Li, Wei Zhang, Shilin Xu. *Effect of binder phases on the microstructure and sliding wear properties of HVOF-sprayed WC-based coatings.* International Journal of Refractory Metals and Hard Materials. Volume 122, August 2024, 106742. https://doi.org/10.1016/j.ijrmhm.2024.106742

[52] Standard test method for measuring abrasion using the dry sand/rubber wheel apparatus, ASTM G65-16, 2021, doi: 10.1520/G0065-16R21.

[53] Standard Test Method for Scratch Hardness of Materials Using a Diamond Stylu, ASTM G171-03, 2017, doi: 10.1520/G0171-03R17

[54] Stosic, N., Smith, I. K., & Kovacevic, A. (2011), *Geometry of screw compressor rotors and their tools*. Journal of Mechanical Engineering Science, 225(1), 125–140.

[55] T.S. Sidhu S. Prakash R.D. Agrawal (2015) *State of the Art of HVOF Coating Investigations— A Review*, Marine Technology Society Journal, Volume 39, Number 2, pp53-64.

[56] Taguchi, G., Chowdhury, S., & Taguchi, S. (2005). Robust Engineering: Learn How to Boost Quality While Reducing Costs & Time to Market. McGraw-Hill.

[57] Vasileios Katranidis, Spyros Kamnis & Sai Gu (2018) *Prediction of Coating Properties of Thermally Sprayed WC–Co on Complex Geometries*". Journal of Thermal Spray Technology, Volume 27, pages 1025 (2018), https://link.springer.com/article/10.1007/s11666-018-0739-6

[58] Vu-Quoc, L., & Zhang, X. (2002), *Modeling the dependence of the coefficient of restitution on the impact velocity in elasto-plastic collisions*. International Journal of Impact Engineering, 23(9), 863–878.

[59] Warren Arthur Nelson (2005), *HVOF bi-layer coating with controlled porosity for use in thermal barrier coatings*. London Patent Operation.

[60] Wenxiang Shu, Xiaofeng Deng, Weiduo Guo, Wei Shi, Shuai Li, Bei Zhang, Jingying Bai (2022). *Microstructure and wear resistance of HVOF sprayed WC-10Co-4Cr coating on Ti-6Al-4V*. Heat treatment and surface engineering 2022, vol. 4, no. 1, 70–75. https://doi.org/10.1080/25787616.2022.2148352

[61] Wu, J., Guo, Y., & Wang, D. (2021), *A numerical study of the dynamic behavior of granular materials in a screw conveyor*. Journal of Engineering and Applied Sciences, 10(3), 112–118.

[62] Y.I. Oka, K. Okamura, T. Yoshida (2005), *Practical estimation of erosion damage caused by solid particle impact. Part 1: Effects of impact parameters on a predictive equation*. Wear, 263(1-6), 330–338.

[63] Y.I. Oka, K. Okamura, T. Yoshida (2005), *Practical estimation of erosion damage caused by solid particle impact. Part 2: Mechanical properties of materials directly associated*. Wear, 263(1-6), 339–346.

[64] Zhu, H. P., Zhou, Z. Y, Yang, R. Y., & Yu, A. B. (2007). *Discrete particlesimulation of particulate systems: Theoretical developments*: Theoretical developments. Chemical Engineering Science, 62(13), 3378–3396.